Clin. Phys. Physiol. Meas., 1991, Vol. 12, Suppl. B, 59–67. Printed in the UK

Josephson junctions and DC SQUIDS based on Nb/Al technology

J Flokstra, D J Adelerhof, E P Houwman, D Veldhuis and H Rogalla

University of Twente, Faculty of Applied Physics, PO Box 217, 7500 AE Enschede, The Netherlands

Abstract. A process for fabricating high-quality Josephson junctions and DC SQUIDs on basis of Nb/Al technology has been developed. DC magnetron sputtering is used for the deposition of the metal layers and the barrier is formed by thermal oxidation of the Al-layer. The junction area of 5 μm × 5 μm is obtained using anodisation. Three types of Josephson tunnel junctions have been prepared: standard Nb/Al, AlO_x/Nb, symmetric Nb/Al, AlO_x, Al/Nb and Nb/Al, AlO_x/AlO_x/Nb, the latter having a double oxide layer. We performed current–voltage and conductance–voltage measurements at different temperatures and special attention was paid to the noise behaviour. Gap and sub-gap parameters as well as barrier parameters are presented. Three different DC SQUID configurations were developed on basis of the Nb/Al Josephson junctions. The measured characteristics of the standard Tesche–Clarke DC SQUID, the resistively shunted SQUID and the inductively shunted SQUID are compared with special attention being paid to the noise properties. A 19-channel DC SQUID magnetometer with standard and/or resistively-shunted DC SQUIDs is under construction.

1. Introduction

Multichannel DC SQUID magnetometers for biomagnetic research have been developed by several research groups and systems with up to 37 channels are already commercially available. Although the clinical value of these instruments has not yet been fully proven, the development of second-generation systems with improved sensors is of great interest. Improvements are possible with respect to, for example, the spectral noise density of the sensor, the signal coupling to the SQUID hole and the SQUID read-out. These subjects are all under study in our group.

In this paper we will describe the ongoing research on the fabrication of high-quality Josephson tunnel junctions based on Nb/Al technology, both for application in SQUID sensors and superconducting x-ray detectors. Several barrier configurations have been prepared and special attention was paid to the sub-gap characteristics and the shape of the potential barrier. The results on the DC SQUIDs will also be presented. We developed three different SQUID structures and the measured characteristics will be compared.

2. Josephson tunnel junctions based on Nb/Al technology

Josephson tunnel junctions based on Nb and Al are usually made by covering the Nb base electrode with a thin Al overlayer that is partly oxidised to form AlO_x. Before the deposition of the Nb counter electrode it may be profitable to cover the AlO_x by a thin Al layer for obtaining a symmetric SNINS (S = superconductor, N = normal

0951-7979/91/0B0059 + 09 $02.50

metal, I = insulator) junction. The reaction between O–H groups at the surface of the AlO_x and the Nb counter electrode, often considered as causing microshorts between the electrodes (Ronay and Latta 1983), is then prevented. We fabricated three types of junctions, standard Nb/Al, AlO_x/Nb, symmetric Nb/Al, AlO_x, Al/Nb and Nb/Al, AlO_x/AlO_x/Nb containing a double oxide layer (Adelerhof *et al* 1991). The thickness of the second Al layer in the SNINS junctions was varied between 1 and 3 nm. The Nb and Al layers were deposited by DC magnetron sputtering, and the thermal oxidation in pure O_2 at various pressures was performed at 10 °C during 1 h. The double AlO_x layer was prepared in two deposition and oxidation steps (Houwman *et al* 1990). The junction areas were defined by the selective niobium anodization process (SNAP) and are 5 μm × 5 μm, 10 μm × 10 μm and 20 μm × 20 μm. A survey of the junctions prepared is given in table 1.

Table 1. The various junction types and configurations.

Junction	Type	Base electrode	Oxidation pressure (mbar)	Counter electrode
3d4	SNINS	Nb + 4 nm Al	267	3 nm Al + Nb
3d5	SNINS	Nb + 4 nm Al	26.7	3 nm Al + Nb
3d6	SNINS	Nb + 4 nm Al	2.67	3 nm Al + Nb
3d15	SNINS	Nb + 3 nm Al	267	2 nm Al + Nb
3d12	SNINS	Nb + 3 nm Al	267	1 nm Al + Nb
3d17	SNIS	Nb + 3 nm Al	267	Nb
3@24	SNIIS	Nb	double oxide AlO_x layer	Nb

The current–voltage ($I - V$) characteristics of the junctions have been obtained with low-noise battery powered electronics. The standard gap parameters, the gap voltage V_g and the (theoretical) maximum critical current density I_{c0}, are presented in table 2.

Table 2. Gap and sub-gap parameters of the junctions. The values represent average values.

Junction	Type	Gap parameters		Sub-gap parameters			
		V_g (mV)	J_{c0}	I_1/I_{c0} (%)		I_2/I_{c0} (%)	
		4.2 K	A cm^{-2}	4.2 K	~ 1.6 K	4.2 K	~ 1.6 K
3d4	SNINS	2.76	44	—	—	3.2–3.5	—
3d5	SNINS	2.77	162	3.0–3.2	0.014–0.13	3.9–4.3	0.68–1.1
3d6	SNINS	2.76	595	3.0–3.1	0.010–0.015	3.8–3.8	0.65–0.71
3d15	SNINS	2.77	40	2.8–3.5	0.010–0.082	3.2–3.7	0.41–0.90
3d12	SNINS	2.83	36	2.7–2.9	0.034–0.042	3.4–4.4	0.62–1.6
3d17	SNIS	2.78	110	3.3–4.9	0.046–1.7	5.1–7.0	1.7–3.7
3@24	SNIIS	2.80	48	—	—	5.4–5.9	—

The sub-gap parameters were determined at various temperatures. The sub-gap currents I_1 at 1 mV and I_2 at 2 mV, relative to the maximum critical current $I_{c0} = J_{c0}A$ (A is junction area), are also given in table 2. The standard quality parameter $V_m (= I_{c0} \times 2\ \text{mV}/I_2)$ at 4.2 K ranges from 45 to 63 mV. The temperature dependence of the sub-gap $I - V$ characteristics is clearly demonstrated in figure 1 for a 5 μm $\times$ 5 μm SNINS junction.

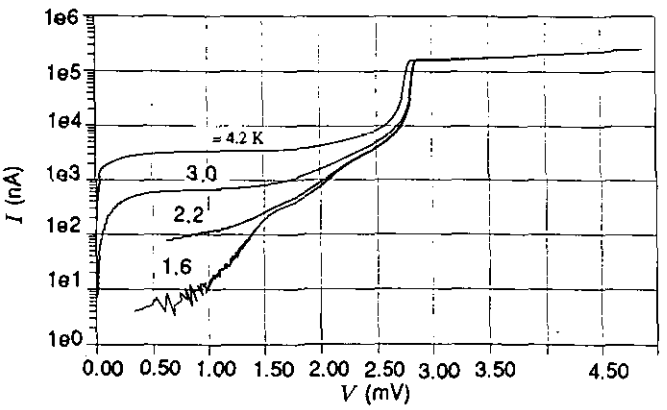

Figure 1. $I - V$ characteristics of a 3d6 junction measured at four different temperatures.

The sub-gap current at 4.2 K is dominated by single-particle tunnelling. This tunnelling is strongly dependent on temperature and leads, at 1.6 K, to currents of the order of 10 nA for this junction. It is seen from figure 1 that an additional tunnel mechanism becomes effective at $Vg/2$, most probably the nearly temperature-independent two-particle tunnelling process proposed by Schrieffer and Wilkens (1963). Although the sub-gap parameters are quite good this two-particle effect is an indication that the homogeneity of the barrier can be still improved.

In order to obtain more information about the potential barrier, conductance–voltage (σ–V) measurements were performed up to 0.5 V using a standard lock-in technique. Experimental σ–V curves for a SNIS, SNINS and SNIIS junction are given for $T = 4.2$ K in figure 2.

The σ–V curve for the SNINS junction is symmetric and parabola-like. The SNIS junction clearly shows deviations from this behaviour especially at the negative voltage side. Furthermore the curve exhibits the occurrence of noise. The σ–V curve for a SNIIS junction has no parabolic shape at all.

The experimental σ–V curves have been fitted with the σ–V behaviour of a trapezoidal barrier with heights $\Phi_{\text{Base Electrode}}$ and $\Phi_{\text{Counter Electrode}}$ and thickness d (Brinkman *et al* 1970). The barrier parameters obtained are presented in table 3.

It is found that the σ–V curves of SNINS junctions can be described by the theory for $|V| > 0.2$ V. The barrier is nearly symmetric but not completely trapezoidally shaped. The σ–V curve of a SNIS junction indicates that the potential barrier is sharp at the counter electrode side and gradually changes behaviour at the base electrode side, similar to SNINS junctions. The σ–V curve of a SNIIS junction could not be described by a trapezoidal barrier at all indicating an inhomogeneous barrier

The noise properties of SNINS and SNIS junctions at 4.2 K have been investigated.

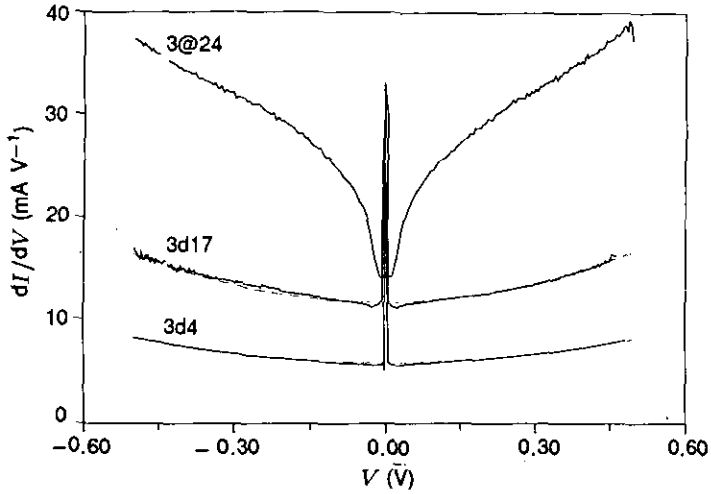

Figure 2. Conductance–voltage (σ–V) characteristics of a SNINS junction (3d4), a SNIS junction (3d17) and a SNIIS junction (3@24). All junctions have dimensions 5 μm × 5 μm.

Table 3. Barrier parameters of the junctions.

Junction	Type	Barrier parameters		
		d (Å)	Φ_{BE} (eV)	Φ_{CE} (eV)
3d4	SNINS	9.1	1.66	1.72
3d5	SNINS	8.6	1.49	1.59
3d6	SNINS	8.0	1.30	1.50
3d15	SNINS	9.7	1.45	1.50
3d12	SNINS	10.1	1.24	1.50
3d17	SNIS	8.8	1.7	1.50
3@24	SNIIS	—	—	—

Clear telegraph noise has been observed in SNIS junctions and to a much lesser extent also in SNINS junctions where the second Al layer is 1 nm. No telegraph noise has been observed in SNINS junctions with a thicker Al layer. This is a strong indication that the telegraph noise is due to trapped states at the Nb/AlO_x interface and clearly a 1 nm thick deposited Al layer is not adequate cover to the AlO_x layer in SNINS junctions completely.

3. DC SQUIDs based on Nb/Al technology

DC SQUIDs often consist of a washer-type SQUID ring containing the two resistively shunted tunnel junctions and a planar input coil on top of the washer. The sensing coils in a neuromagnetometer have an inductance in the range 0.5–2 μH and impedance matching between sensing coils and input coil has to be realised by a large number of turns of the input coil in case of a standard DC SQUID configuration. Such a planar coil introduces a large shunt capacitance across the SQUID loop and together with the washer forms a stripline resonator. The large number of input turns

may therefore be responsible for a considerable amount of excess noise leading to SQUID performance degradation.

We developed various DC SQUID sensor configurations in order to obtain more freedom in the choice of the number of input turns (Houwman *et al* 1991). Apart from the standard type SQUID, so-called large β SQUIDs were designed facilitating the signal coupling. It concerns resistively and inductively shunted SQUIDs. The resistively shunted SQUID has a shunt resistance across the SQUID loop. The inductively shunted SQUID has an additional inductance loop with large area coupled to the small SQUID loop. The sensing coil is coupled to an input coil on the large loop.

The maximum voltage modulation depth, ΔV_m, is approximately equal to $I_0 R/(1+\beta)$ for the standard type SQUID, with I_0 the critical current of one junction, R the shunt resistance of the junction and β the screening parameter $2L_1 I_0/\Phi_0$, with L_1 being the SQUID inductance and Φ_0 the flux quantum. Standard SQUIDs are designed with $\beta \approx 1$. ΔV_m of the resistively and inductively shunted SQUIDs is not strongly dependent on β and equals $I_0 R/2$. The spectral flux-noise density is in all three cases proportional to β^2 so that large β SQUIDs are less sensitive. The coupling is, however, facilitated and a reduction in the excess noise may be expected. Therefore the noise balance may become positive.

The DC SQUIDs were fabricated on the basis of our junction technology. The junctions, with critical currents in the range from $5-15$ μA, are shunted by thin-film Pd resistors to obtain β_c values of 0.1–0.5. The insulation between washer and input coil is realised by a double SiO_2 layer. The second layer is deposited with negative voltage bias for planarisation reasons.

The design parameters of the various SQUID configurations are given in table 4 for two standard SQUIDs, Sta1-2, four resistively shunted SQUIDs, Res1-4, and two inductively shunted SQUIDs, Ind1-2. The junctions of Sta1-2 are placed at the inside of the washer to avoid the parasitic slit inductance. The junctions of the resistively shunted SQUID are placed at the outside of the washer. A picture of the inductively shunted SQUID is given in figure 3. A small washer with the junctions at the inside is coupled to the modulation coil. The washer is attached to a large washer loop carrying the input coil.

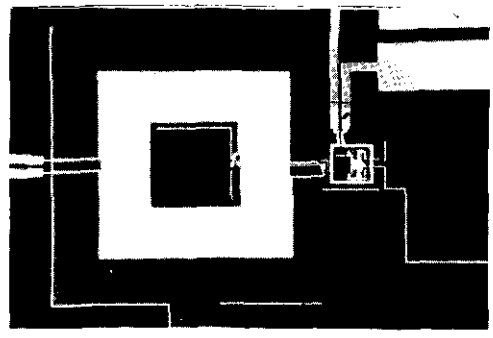

Figure 3. Photograph of the inductively shunted SQUID (type Ind1 of table 4) with the small loop interrupted by the junctions and a large loop carrying the input coil. The modulation coil (1 turn) is around the small hole. There is a narrow slit in the large washer from the large hole and ending on the superconducting shunt, formed by part of the small loop. This slit contains the return line of the input coil.

Table 4. Various DC SQUID configurations. Calculated and experimental results.

SQUID	Design										Experimental results		
	SQUID loop			Large loop				Input coil		Coupling input coil to SQUID (nH)	SQUID L_1 (pH)	Coupling input coil to SQUID (nH)	Coupling factor k_{12}
	Hole (μm)	L_{hole} (pH)	L_{slit} (pH)	Hole (μm)	L_{hole} (pH)	L_{slit} (pH)	L_{sh} (pH)	Turns	L_{input} (μH)				
Sta1	70	110	—	—	—	—	—	29	0.095	3.1	150	2.2	0.58
Sta2	145	230	—	—	—	—	—	21	0.10	4.7	270	4.1	0.79
Res1	150	240	136	—	—	—	—	21	0.11	5.0	385	5.2	0.8
Res2	300	470	153	—	—	—	—	21	0.21	9.9	670	—	—
Res3	750	1330	102	—	—	—	—	13	0.23	15	1480	—	—
Res4	1500	2980	85	—	—	—	—	10	0.31	24	3100	—	—
Ind1	70	110	—	300	470	136	18	21	0.21	0.29	160	0.29	0.050
Ind2	70	110	—	1500	3100	68	18	10	0.32	0.18	160	0.29	0.024

Apart from the SQUID hole size and the self-inductances of loop and slit, table 4 contains the information about the input coil and the coupling from input coil to SQUID. Experimental results on input coil inductance, input coil coupling to SQUID are also presented.

The I–V and V–Φ characteristics of all the SQUIDs produced are generally smooth in the normal bias range up to about (3–4)I_0 where the first cross over in the I–V curves is present.

The spectral densities of the flux noise of various SQUIDs with open input coil were measured in a standard 100 kHz flux-locked loop with square wave flux modulation. The white noise level according to theory and the measured values are given in table 5. The values differ by a factor 2 to 8.

Table 5. Flux and field noise sensitivity of various SQUIDs. Two samples of Sta1 and Sta2 type SQUIDs are given. SQUID Res 2 had a short-circuited input coil. Accounting for this effect a field noise of about 0.6 fT $Hz^{-1/2}$ can be expected.

SQUID	Flux noise ($\times 10^{-6}\Phi_0$ $Hz^{-1/2}$)		Field noise B_n (fT $Hz^{-1/2}$)
	$\Phi_{n,\,\text{theory}}$	$\Phi_{n,\,\text{exp.}}$	
Sta1	1.2	3.8	3.5
Sta1	1.2	8.4	7.8
Sta2	2.1	10	5.0
Sta2	1.9	15	7.5
Res2	1.2	2.6	1.7
Ind1	1.6	3.5	28
Ind2	1.2	1.8	27

The spectral densities for two standard type SQUIDs are given in figure 4. It is seen that the onset of the $1/f$ noise takes place at about 1 Hz.

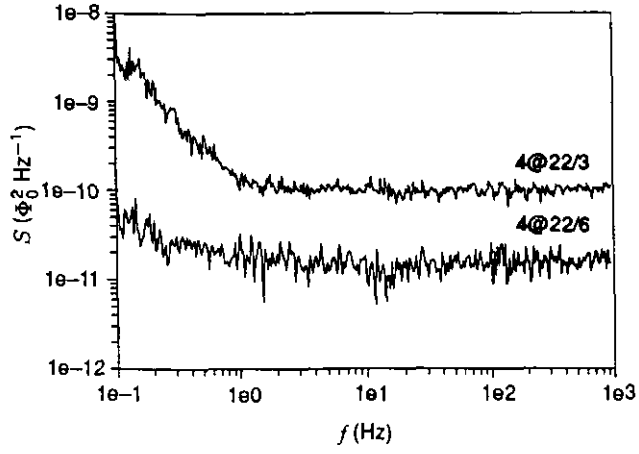

Figure 4. Flux-noise spectral densities of two standard SQUIDs.

The field noise is calculated in case the SQUID is connected to a wire-wound first-order gradiometer, having two sections of 3 turns each with a diameter of 20

mm and a base line length of 40 mm. The self-inductance for the sensing coil is then about 0.83 μH. The field noise for standard and resistively shunted SQUIDs is of the order of 1–8 fT $Hz^{-1/2}$ which is adequate for detecting the very small brain fields. The field noise level of the inductively shunted SQUID is much higher due to the poor coupling between the large loop and the SQUID hole. This SQUID type is not adequate in this configuration for use in the neuromagnetometer, but probably will prove valuable in high T_c SQUID configurations.

4. Concluding remarks

We developed a process for fabricating high-quality Josephson tunnel junctions and DC SQUIDs. On basis of the results for the various junction structures and DC SQUID configurations, we prepared Res1 and Sta2 type DC SQUIDs with SNINS junctions. The number of turns of the input coils in both cases is 21. The white-noise level is typically 3×10^{-6} Φ_0 $Hz^{-1/2}$ for Res1 and 1×10^{-5} Φ_0 $Hz^{-1/2}$ for Sta2. These SQUIDs will be used in the 19-channel DC SQUIDS neuromagnetometer (ter Brake *et al* 1991).

References

Adelerhof D J, Houwman E P, Fransen P B M, Veldhuis D, Flokstra J and Rogalla H 1991 Characterization of different types of Nb-AlOx based Josephson tunnel junctions *IEEE Trans. Magn.* **MAG-27** 3153–6

ter Brake H J M, Flokstra J, Jaszczuk W, Stammis R, Van Ancum G K, Martinez A and Rogalla H 1991 The UT 19-channel DC SQUID based neuromagnetometer This volume pp 45–50

Brinkman W F, Dynes R C and Rowell J M 1970 Tunneling conductance in asymmetrical barriers *J. Appl. Phys.* **41** 1915–21

Houwman E P, Veldhuis D, Flokstra J and Rogalla H 1990 Fabrication and properties of Nb/Al, AlO_x/Nb Josephson tunnel junctions with a double oxide barrier *J. Appl. Phys.* **67** 1992–4

Houwman E P, Veldhuis D, Flokstra J, Ter Brake H J M, Jaszczuk W, Martinez A and Rogalla H 1991 DC SQUID sensor system for multichannel neuromagnetometry *IEEE Trans. Magn.* **MAG-27** 2955–8

Ronay M and Latta E E 1983 Interaction of niobium counter electrodes with aluminum oxide and rare-earth oxide tunnel barriers *Phys. Rev.* B **27** 1605–9

Schrieffer J R and Wilkens J W 1963 Two-particle tunnelling processes between superconductors *Phys. Rev. Lett.* **10** 17–20